IEEE Access
Multidisciplinary | Rapid Review | Open Access Journal

Received 15 June 2024, accepted 28 July 2024, date of publication 8 August 2024, date of current version 30 August 2024.

Digital Object Identifier 10.1109/ACCESS.2024.3440577

RESEARCH ARTICLE

Improving Early Detection and Classification of Lung Diseases With Innovative MobileNetV2 Framework

AMRITA TRIPATHI[1], TRIPTY SINGH[1], (Senior Member, IEEE), REKHA R. NAIR[2], (Member, IEEE), AND PRAKASH DURAISAMY[3], (Senior Member, IEEE)

[1]Department of Computer Science and Engineering, Amrita School of Computing, Amrita Vishwa Vidyapeetham, Bengaluru 560035, India
[2]Department of Computer Science and Engineering, Alliance School of Advanced Computing, Alliance University, Bengaluru 562106, India
[3]Department of Computer Science, University of Wisconsin–Green Bay, Green Bay, WI 53706, USA

Corresponding author: Tripty Singh (tripty_singh@blr.amrita.edu)

ABSTRACT Any condition that damages or impedes the normal operation of the lungs is classified as a lung disease, and failure to identify and address it early can potentially lead to false outcomes. To address this challenge, two innovative techniques are proposed for lung disease classification, supporting medical professionals in diagnosing and providing preventive measures at an early stage. The Proposed Model 1 integrates a custom MobileNetV2L2 architecture, that builds upon the MobileNetV2 framework through fine-tuning and customization. This model enhances performance by incorporating a ridge or L2 Regularizer within its dense layer. The Proposed Model 2, custom CNN2 built on CNN as its foundational block, is fine-tuned with ELU as the activation function, replacing ReLU, and incorporates the ridge or L2 regularization technique. The proposed research utilizes two publicly available datasets: DS1(Data Set1), which is the Lung Disease 5-class dataset, and DS2(Data Set2), which is the Lung Disease 4-class dataset and is collected from Kaggle. In comparison to cutting-edge methods like EfficientNet B0, InceptionV3, ResNet, and InceptionResNetV2, the Proposed Model 1's outcomes perform better. It attained 100% validation accuracy, 99.53% training accuracy, and 95.51% test accuracy. Proposed Model 2 achieved testing accuracy of 99.26%, validation accuracy of 91.56%, and training accuracy of 96.79%, the suggested Proposed Model 2 performs quite well. As a supplementary opinion during the diagnostic process, the proposed research is a useful tool for pulmonologists.

INDEX TERMS Convolutional neural networks, contrast limited histogram equalization technique, DenseNet, InceptionV3, InceptionResNetV2, MobileNetV2, L2 Regularizer.

I. INTRODUCTION

The third most significant cause of death worldwide, according to statistics, is lung disease [1]. The function of the lungs is to take oxygen inside and remove carbon dioxide. If any part of the lung is not working correctly, lung diseases arise.

Modalities used by radiologists to detect lung diseases are X-ray and Computed Tomography(CT) techniques, but X-ray is more economical than CT scans; thus, radiologist suggests X-ray more frequently for primary diagnosis of lung disease [2]. Artificial Intelligence (AI) aims to replicate human cognitive processes, catalyzing a transformative shift in healthcare. This evolution is due to increased analytics tools and abundant healthcare data, facilitating automated diagnoses across various diseases such as cancer, COVID-19, and pneumonitis. Numerous models have recently emerged in response to this trend [3] Artificial intelligence in the health area happened for the first time in 1950 when researchers utilized computers to improve disease diagnosis.

The associate editor coordinating the review of this manuscript and approving it for publication was Cesar Vargas-Rosales.

In recent times, the use of AI in the medical field has increased due to high computing power machines and a vast amount of data available in digital form [3] The increased volume of image data presents new demands for analysis and processing. Convolutional neural networks were specifically developed to address these challenges. Their robust image classification and identification capabilities have found widespread applications across various image classification systems [7].

The main aim of the proposed research work is to create an automated deep-learning framework application for quick and precise identification and categorization of lung diseases such as Tuberculosis, Viral Pneumonia, COVID-19 and Bacterial Pneumonia. The proposed research utilizes two publicly available data sets to achieve this aim. Dataset 1, DS1 includes 10,000 X-ray images of five classes of lung diseases, such as regular X-rays with Viral Pneumonia, Tuberculosis, COVID-19, and Bacterial Pneumonia. Dataset 2, DS2 includes 8,107 X-ray images of three lung diseases, such as regular X-rays with COVID-19, Pneumonia and Tuberculosis. Two deep-learning models are proposed here to create an automated deep-learning framework. The first proposed deep learning model (MobileNetV2L2) provides denoising of the raw image datasets using the Contrast limited image enhancement technique (CLAHE) and then the MobileNetV2 transfer learning technique provides categorization of the specified lung diseases. To enhance the model performance and to avoid overfitting L2 or Ridge regularization technique is added to this framework. This proposed model is also compared with other existing models namely Shallow CNN, VGG19, EfficientNetB0, InceptionV3, ResNet50, DenseNet121, Xception, MobileNet and InceptionResNetV2. The second Proposed deep learning model framework consists of three convolutional layers and three dense layers with ELU as an activation function. To enhance the model performance and to provide categorization of specified lung diseases, the proposed framework applies dropout and Ridge or L2 Regularizer in its dense layer.

The remaining part of the paper consists of a detailed literature review described in Section II and the methodology proposed in Section III. The research result and analysis are in Section IV followed by the conclusion and the future scope of the work in Section V.

II. LITERATURE REVIEW

Deep learning algorithms have recently gained popularity because they can identify anomalies in chest X-ray images [1]. Studies have shown consistent and effective results when artificial intelligence is used to assist in diagnosis [3]. In the task related to lung disease multi-classification, a lot of work happened using various transfer learning techniques [1], [11], [14], [16]. In the paper [1] lung diseases multi-classification of 10 lung diseases (Effusion, COVID-19, Tuberculosis, Lung Opacity,Pneumonia Mass, Nodule, Pneumothorax, and Pulmonary Fibrosis, along with the Normal class) is done using the LungNet22 model which is built upon performing ablation study on basic building blocks of VGG16 architecture after pre-processing the dataset with contrast limited adaptive histogram equalization (CLAHE) and eight augmentation techniques, LungNet22 achieved a nice accuracy of 98.89% [1]. In the paper [16] KarNet framework by itilizing transfer learning models is proposed to classify COVID-positive and COVID-negative classes using computed tomography images. The KarNet framework is developed using pre-trained models of DenseNet201, VGG16, ResNet50V2, and MobileNet as its basic blocks. The KarNet framework with DenseNet201 showed nice performance with the accuracy of the test dataset as 97% [16]. Few papers [1], [7] provided image pre-processing in the form of either denoising the image or applying any image enhancement techniques before applying the dataset to deep learning models and achieved commendable results. In the paper [7] author proposed image enhanced model using k-symbol Lerch transcendent functions which enhances the images based on image pixel probability. After the image enhancement step, the customized CNN architecture and two pre-trained CNN models AlexNet, and VGG16 are developed. The proposed model classifies Pneumonia, Normal, and COVID disease X-ray and CT scan images showing classification accuracy, sensitivity, and specificity of 98.60%, 98.40%, and 98.50% for the X-ray image dataset respectively, and 98.80%, 98.50%, 98.40% for the CT scans dataset, respectively [7]. In [2] author proposed a unique deep-learning model to provide a classification of lung diseases. Here image pre-processing is performed using optimal filtering, Feature extraction is performed using 2DCNN, and the classification of the lung diseases is performed by classifying the CNN features using the different machine learning classifiers such as AdaBoost, Support Vector Machine (SVM), Random Forest (RM), Backpropagation Neural Network (BNN), and Deep Neural Network (DNN). Propose model Hybrid deep learning algorithm framework provides better results [2]. Many researchers explored binary classification of lung-related diseases. In the paper [9] research work is carried out to provide an efficient Tuberculosis disease detection framework. This proposed framework utilizes transfer learning techniques with and without segmentation techniques. It is shown that segmented X-ray images are performing better with the DenseNet201 transfer learning technique. The classification accuracy, precision, and recall of Tuberculosis disease classification without segmentation are 96.47%, 96.62%, and 96.47% and with segmentation are 98.6%, 98.57%, and 98.56% respectively. It is seen here that the image segmentation technique is improving performance [9], [25]. Few paper are providing customized CNN to classify lung diseases [12] In paper [12] author proposed customized CNN approach naming the model as DarkCovidNet for binary classification of COVID or non COVID and multiclass classification of COVID, Normal and Pneumonia disease is performed. The classification

accuracy of 98.08% for binary class and 87.02% For multi-classification case is achieved in this work [12]. In paper [26] author utilized a hybrid deep-learning framework to classify lung diseases. Here hybrid deep learning framework which is a combination of VGG, data augmentation, and spatial transformer network (STN) with CNN which is named VDSNet [26]. Few papers [45], [50], [54] are showing the significance of MobileNet transfer learning techniques In paper [50] MobileNetV2 architecture significance is discussed. Introduced ''Exponential linear unit'' activation function to implement faster and more accurate deep learning models [55]. Using the identity for positive values, ELU eliminates the vanishing gradient problem. ELU has got negative values which helps mean unit activation nearer to zero. ELU activation function is also becoming beneficial in a few applications as per the literature survey [55] The literature gap that is identified with this literature survey is as follows:

- Many papers have neglected to explore certain image pre-processing techniques for the specified dataset
- There are very few works available that specifically utilize the DS2 dataset.
- Few of the works have included validation accuracy as one of their performance metrics.
- No work on the specified dataset has employed regularizers to avoid the risk of model overfitting.

So a generalized automated framework for providing classification of lung disease is proposed for the rapid and accurate diagnosis and classification of lung diseases, including COVID-19, Tuberculosis, Bacterial pneumonia, Viral pneumonia, and healthy cases. The objectives of our work are as follows:

- To develop innovative techniques for accurate lung disease classification, assisting medical professionals in early diagnosis and preventive measures
- To propose Model 1, which integrates a custom MobileNetV2L2 architecture built upon the MobileNetV2 framework with fine-tuning, customization, and the incorporation of a ridge or L2 regularizer within its dense layer to enhance performance
- To propose Model 2, which is built on a convolutional neural network (CNN) as its foundational block, fine-tuned with the Exponential Linear Unit (ELU) activation function replacing ReLU, and incorporating the ridge or L2 regularization technique
- To evaluate the proposed models using two publicly available datasets: DS1 (Lung Disease 5-class dataset) and DS2 (Lung Disease 4-class dataset) collected from Kaggle
- To achieve superior performance in lung disease classification compared to state-of-the-art techniques like EfficientNet B0, InceptionV3, ResNet, and Inception-ResNetV2
- To provide a valuable tool for pulmonologists, offering a secondary opinion in the diagnostic process by leveraging the proposed models' accurate classification capabilities

III. PROPOSED METHODOLOGY

This section comprises of four modules as shown in Figure. 1 such as Image dataset, Image Pre-processing, Deep Learning models, and Hyperparameter tuning. The description of each part is given below.

A. IMAGE DATASET

The dataset utilized for the proposed work is the lung disease dataset which is collected from the Kaggle website [59], [60]. Dataset 1, DS1 includes 10,000 X-ray images of five classes of lung diseases, such as regular X-rays with Viral Pneumonia, Tuberculosis, COVID-19, and Bacterial Pneumonia. Dataset 2, DS2 includes 8,107 X-ray images of three lung diseases, such as regular X-rays with COVID-19, Pneumonia and Tuberculosis. The images included in the dataset comprise of similar size and are categorized into train, test, and validation folders. DS1 dataset is divided into 6054 images as training, 2025 images as testing, and 2016 images as validation as shown in Figure. 2. As illustrated in Figure.3, the DS2 dataset is split into 4861 images for training, 1625 images for testing, and 1620 images for validation. The visualization of the number of images in training, validation and testing folders for DS1 are shown in Figure. 4, Figure. 5 and Figure.6. The distribution of images across the training, validation, and testing datasets for DS2 is visually represented in Figure 7, Figure. 8 and Figure. 9.

B. IMAGE PRE-PROCESSING TECHNIQUES

1) IMAGE RESIZE

The images are resized to 224 × 224 dimensions for the deep learning model to maintain uniformity in input dimensions. This helps ensure consistency and facilitate the model's processing.

2) IMAGE AUGMENTATION

The problem of inadequate data can be addressed using data augmentation technique [10]. Enhancing the size and quality of training datasets to enable the creation of improved deep-learning models is known as data augmentation [10]. To produce Deep Learning models that are effective, the validation error must decrease with the training error [10]. In this work augmentation is done using geometric transformation.

3) HISTOGRAM EQUALIZATION TECHNIQUE

An image enhancement technique known as Contrast Limited Adaptive Histogram Equalization (CLAHE) is employed to improve the contrast of the images. CLAHE technique perform the enhancing of the image by dividing each picture into contextual parts which are known as tiles and generating a histogram for each tile separately and again intensity level

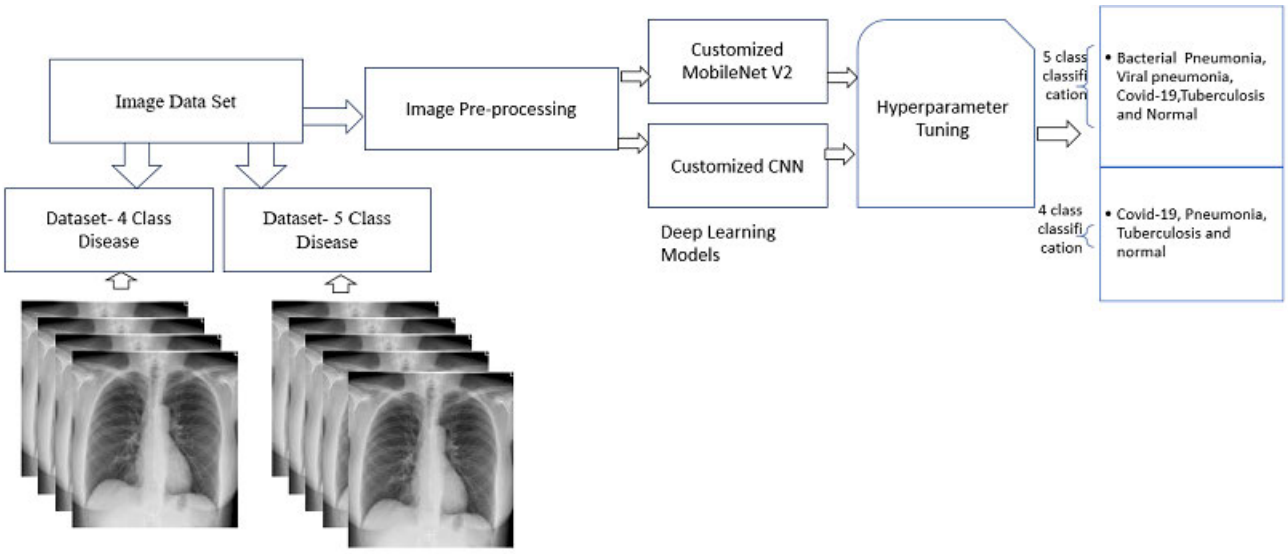

FIGURE 1. Proposed flow of work.

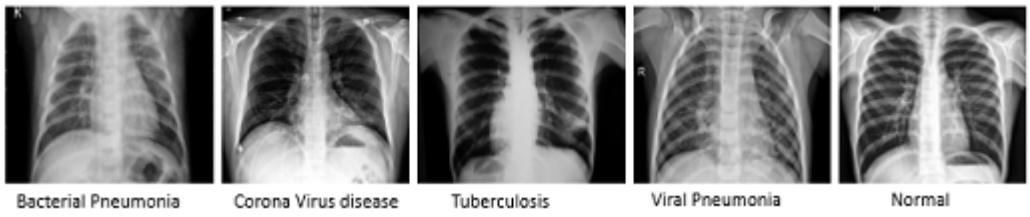

FIGURE 2. Lung diseases dataset DS1 xray images.

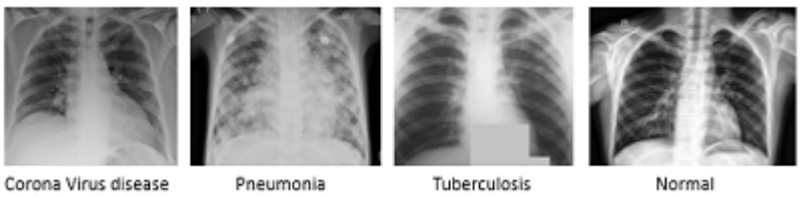

FIGURE 3. Lung diseases dataset DS2 xray images.

change occurs to enhance the quality of the image. [1].

$$N = I \cdot I \div i \cdot i \tag{1}$$

$$l_c = I_{cl} \cdot I_{avg} \tag{2}$$

$$I_{avg} = I_x \cdot I_y \div I_g \tag{3}$$

In above equations N is quantity of tiles generated, I is size of an image in a pixel,i is size of a tiles in pixels, l_c is clip limit, I_{cl} is normalized contrast limit, I_{avg} is the average counts of pixels in the pictureI_x,I_y, I_g represents pixel size in x direction, pixel size in y direction and number of gray scale respectively.

C. DEEP LEARNING MODELS

The initial proposed approach involves applying the Contrast Limited Adaptive Histogram Equalization (CLAHE) technique to enhance the contrast of the image datasets. Subsequently, the enhanced image datasets, processed using the CLAHE technique, are fed as input to eight existing deep-learning models, three customized DenseNet models, and two customized MobileNet models for both the DS1 and DS2 datasets. The first proposed work was carried out with models shallow CNN, VGG19, InceptionV3, EfficientNetNetB0, ResNet50, Xception and MobileNetV2.In comparison to other deep learning techniques with and without applying the CLAHE technique. All the utilized deep learning models worked better after applying the CLAHE technique as MobileNetV2 performed better so to obtain an efficient and reliable deep learning model, MobileNetV2 is customized, ablation study is performed and an L2 regularization technique is added to customized MobileNetV2 to reduce overfitting of the model. The second proposed work is a customized CNN approach where three convolutional layers and three dense layers with an ELU activation function model

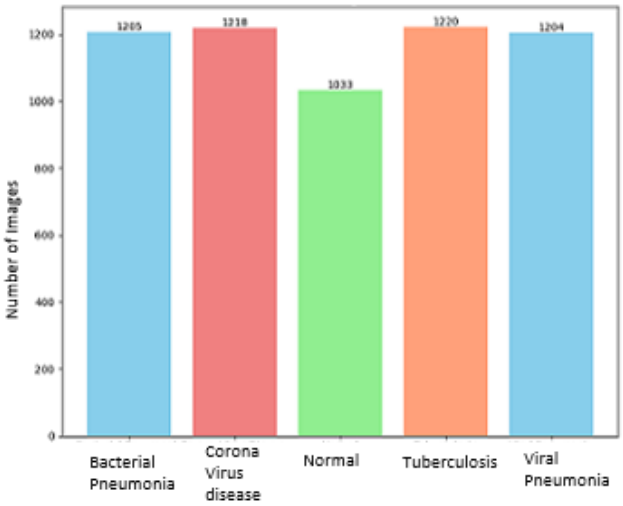

FIGURE 4. The training set data distribution for DS1.

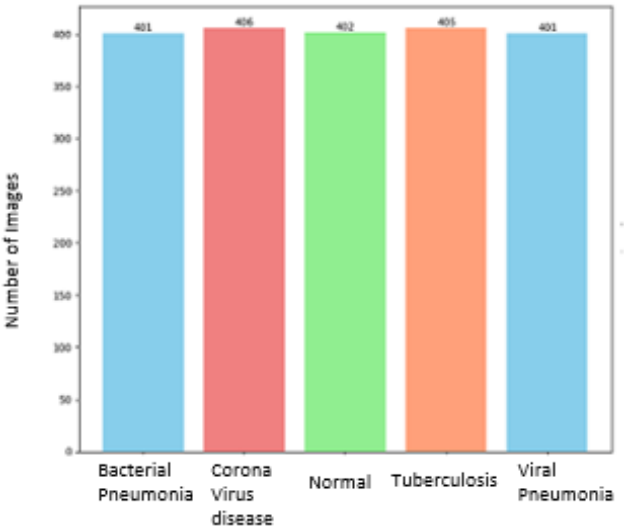

FIGURE 5. The validation set data distribution for DS1.

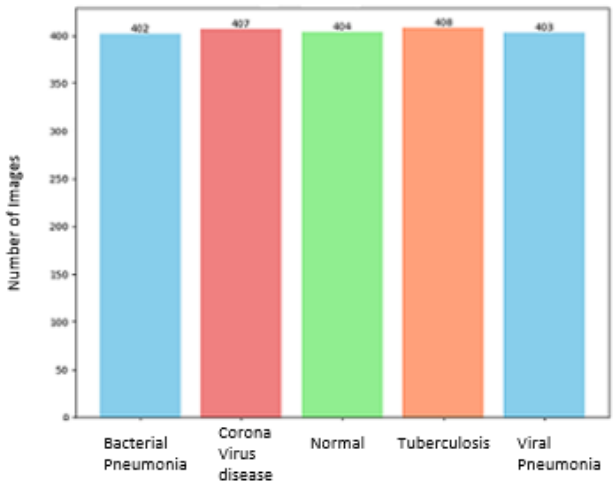

FIGURE 6. The testing set's data distribution for DS1.

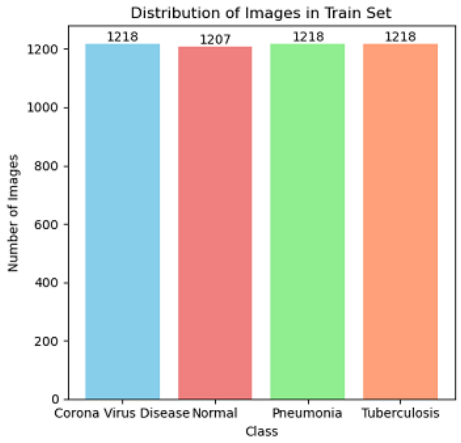

FIGURE 7. Data distribution of the training set for DS2.

are performing better. To reduce overfitting of the model L2 Regularizer is added in the proposed model. Table 1 and Table 2 show training and validation accuracy of DS1 without and with applying CLAHE technique. It is visible from two tables that the MobileNet deep learning technique is showing better performance in comparison to other predefined deep learning techniques.

1) HYPERPARAMETER TUNING

Hyperparameter Tuning is performed to achieve efficient and reliable deep-learning models. For obtaining Proposed Model 1, the Transfer learning approach is utilized, and various experiments are done to obtain our Proposed Model 1. In the first experiment, the DS1 image dataset is given as input to the Contrast Limited Adaptive Histogram Equalization (CLAHE) technique module to provide enhanced quality images. After this step CLAHE enhanced images are given as input to the eight existing deep learning models, 3 customized Densenet models and two customized MobileNet models. 1 and 2 To evaluate the significance of the CLAHE technique to be added before deep learning models, the Chest X-ray image dataset is compared with and without applying the CLAHE technique. Table 1 and Table 2 show the performance of deep learning models without and with the CLAHE technique respectively. After evaluating and observing thirteen deep learning models eight existing and 4 customized transfer learning approaches with and without applying the CLAHE technique, it is observed that after applying the CLAHE technique all the specified deep learning models are performing better. It is also seen in the experiment that MobileNetV2 is performing better in comparison to other specified models 1 and 2

3 is showing training and validation accuracy of all the specified deep learning models for DS2 dataset.

Another Ablation study is done with change in epochs and evaluating the performance of MobileNetV2 to achieve suitable epoch for Proposed Model 1 which is shown in Table 4.

FIGURE 8. Data distribution of the Validation set for DS2.

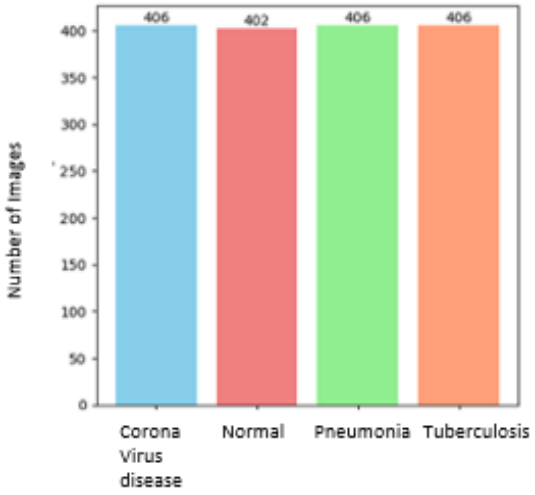

FIGURE 9. Data distribution of the test set for DS2.

2) MODIFIED MOBILENET

The MobileNet class of efficient models is most appropriate for embedded and mobile vision applications. Depth-wise separable convolution is the foundation of MobileNet architecture, is essentially a factorized convolution that factors a conventional convolution into a pointwise convolution (1×1) and a depth-wise convolution [46]. In the MobileNet architecture, the depth-wise convolution applies a single filter to each input channel independently. The outputs are then combined using a 1×1 convolution after the point-wise convolution. A separate layer for filtering and a separate layer for combining were broken apart by the depth-wise separable convolution. The result of this factorization is a significant reduction in computation and model size. Among other deep learning techniques, MobileNet technique is showing better performance so it is modified to achieve commendable performance [46]. Experimentation is done to obtain L2 Regularization weight to achieve efficient performance of proposed model 1. The Rgularization weights was varied from.01 to.000001 and it is observed that Ridge or L2 Regularizer.001 weight is most suitable for the model.

3) CUSTOMMOBILENET1

This Modified Deep Learning model utilizes the MobileNet transfer learning approach with one extra dropout layer of 0.50 to avoid overfitting. To build a more efficient Deep learning model, two additional dense layers are added, one with 512 neurons and an activation function as ReLU. In contrast, the other Dense layer is used for classification purposes with Softmax as the activation function. Custommobilenet1 training and validation accuracy results are shown in Table 7 and Table 8.

4) CUSTOMMOBILENET2

With one layer with 0.50 dropout and five additional dense layers utilized to extract more specific information from the image, the proposed Modified Deep Learning model makes use of the state-of-the-art modified MobileNet transfer learning technique. 512 neurons with Relu as an activation function make up the first dense layer. The proposed model architecture consists of the following dense layers: The second dense layer employs 256 neurons and incorporates the Rectified Linear Unit (ReLU) as its activation function. The third dense layer utilizes 128 neurons and also employs ReLU as the activation function. The fourth dense layer incorporates 64 neurons and incorporates a ridge regularizer to prevent overfitting. Here, 01 weight is added to prevent overfitting. Fifth and last dense layer is for classification purpose and it is using Softmax as an activation function. Custommobilenet2 performance metrics are shown in table7 and Table 8.

An ablation study is done to change in number of dense layers from 2 to 5, freezing other layers of the MobileNetV2 transfer learning approach without adding Regularizer in its dense layer.

In the table 5, it is seen that three dense layer with customized MobileNetV2 is showing better performance Another Ablation study is done with fixing dense layer number as 3 and adding Regularizer different weights and observing the performance.

Various Ablation study is done to obtain the Proposed Model 1 MobileNetV2L2 such as changing number of dense layers which is shown in Table 5 and in Table 6 it is seen that with addition of L2 regularizer with 0.01 weight customized MobileNetV2 with three dense layer is showing commendable performance.

5) CUSTOMDENSENET1

This Modified Deep Learning model utilizes the DenseNet transfer learning approach with one extra dropout layer of 0.50 to avoid overfitting. To create a more efficient Deep Learning model, two extra dense layers are added, one with 512 neurons and an activation function known as ReLU. In contrast, the other Dense layer is used for classification purposes with Softmax as the activation function. CustomdenseNet1 training and validation accuracy results are shown in Table 1 and Table 2.

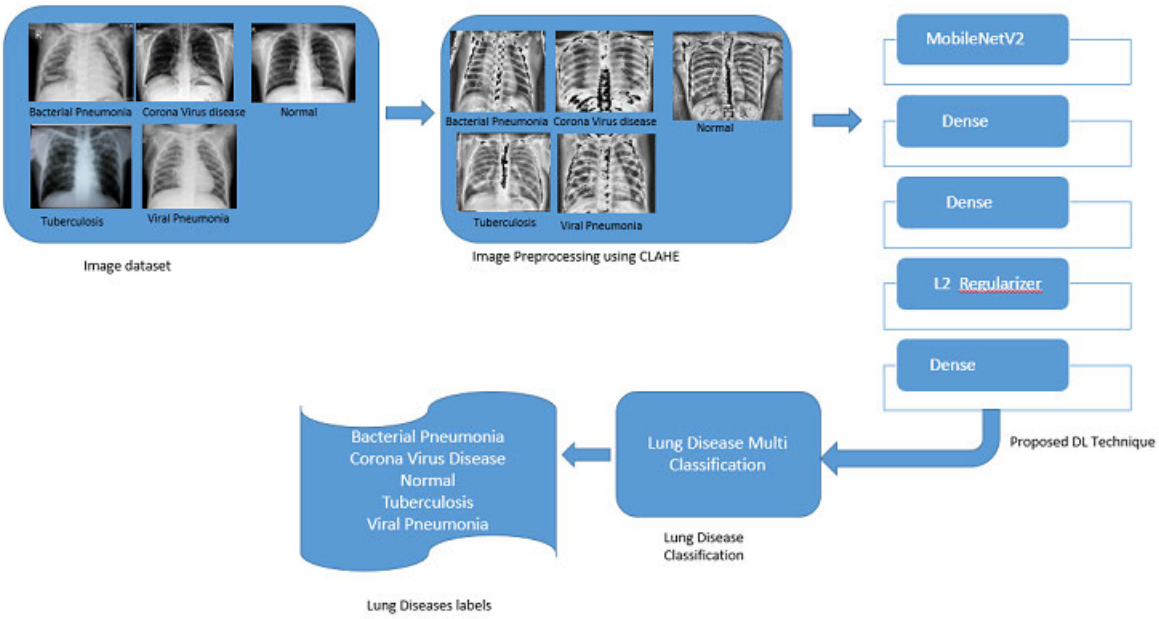

FIGURE 10. Architecture of proposed methodology 1 for MobileNetV2L2.

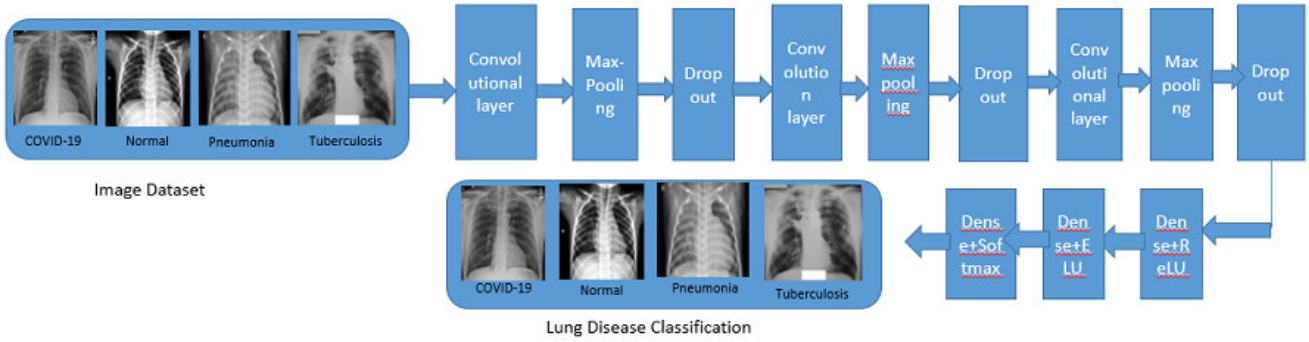

FIGURE 11. Architecture of proposed methodology 2 for Custom CNN2.

6) CUSTOMDENSENET2

This Modified Deep Learning model utilizes the DenseNet transfer learning approach with one extra dropout layer of 0.50 to avoid overfitting. To construct a more robust deep learning model, three additional dense layers are incorporated into the architecture: a second dense layer consisting of 128 neurons and an L2 or ridge regularizer with a value of 0.01 to mitigate overfitting, followed by a third dense layer comprising 512 neurons, utilizing the Rectified Linear Unit (ReLU) as the activation function. In contrast, the other Dense layer is used for classification purposes with Softmax as the activation function.CustomdenseNet2 training and validation accuracy results are shown in Table 1 and Table 2.

7) CUSTOMDENSENET3

This Modified Deep Learning model utilizes the customized DenseNet transfer learning state of the art technique with one layer of 0.50 dropout and additional five dense layer is used for extracting more detailed information from the image. The model architecture comprises the following dense layers: The first dense layer utilizes 512 neurons and incorporates the Rectified Linear Unit (ReLU) as the activation function. The second dense layer employs 256 neurons and also leverages ReLU as the activation function. The third dense layer consists of 128 neurons, again employing ReLU for activation. The fourth dense layer incorporates 64 neurons and incorporates a ridge regularizer with a weight of 0.01 to prevent overfitting and improve generalization. Fifth and last dense layer is for classification purpose and it is using Softmax as an activation function. CustomdenseNet3 training and validation accuracy results are shown in Table 1 and Table 2. Table 7 and Table 8 shows all the performace metrics for DS1 and DS2 datasets. Fig. 16 shows graphical representation of training, validation and test accuracy for CustomdenseNet1, CustomdenseNet2 and CustomdenseNet3 respectively. Various ablation studies are done to achieve a better-performing deep learning model.

Table 7 and Table 8 is showing all the performance metrics of utilized deep learning models for both datasets DS1 and DS2

An ablation study is done to achieve number of dense layer added by fixing activation function and regularization weights. It is observed that Customized CNN with three layers is showing better performance. Another Ablation study is done to check suitable activation function for the proposed model 2. Table 9 is showing Custom CNN 1 model with three dense layer and in the second dense layer ReLU activation function and L2 Regularizer with.01 weight is employed and performance is evaluated with changing numer of epoch as 50, 100, 150 and 200.

Table 9 and Table 11 shows all the performance metrics for a specified dataset for Proposed Model 2 Custom CNN2.

D. PROPOSED STATE OF ART TECHNIQUE

In the research, two state-of-the-art techniques were proposed: one employs Convolutional Neural Networks (CNNs) as its foundational building blocks, while the other utilizes transfer learning. Both models offer innovative solutions within the context of the study. [49]

1) PROPOSED MODEL1

Proposed Model 1 architecture is shown in Figure. 10. The model efficiency is enhanced by adding three additional dense layers and freezing all other layers, thereby adapting the MobileNetV2 transfer learning approach. To avoid overfitting, a dropout rate of 50% and Ridge or L2 regularization with a coefficient of 0.01 is employed. Additionally, a Softmax activation layer is used in the final dense layer to aid in the multi-classification of particular lung diseases. This customized model undergoes training for 150 epochs, yielding impressive results indicative of its state-of-the-art performance. The novelty of the Proposed Model 1 is its customized MobileNetV2 transfer learning approach with the addition of three dense layers and freezing of all other layers. To avoid overfitting of the model Ridge or L2 Regularizer with.01 weight is added to the framework. MobileNet was created especially for contexts with limited resources and mobility. MobileNet advances the state of the art for customized computer vision models by using a smaller amount of memory and processes while maintaining the same level of accuracy. This can be seen from the equations given below The standard convolution computation cost is given in the below equation

$$C = K_l \cdot K_l \cdot X \cdot Y \cdot K_f \cdot K_f \tag{4}$$

where $K_l \cdot K_l$ is kernel size, $K_f \cdot K_f$ is feature map size, X is number of input channel, Y is number of output channel. Depthwise seperable convolution cost is given by below equation

$$C = K_l \cdot K_l \cdot X \cdot K_f \cdot K_f \tag{5}$$

By using two step process of convolution in the MobileNet approach total computation cost of the parameters reduces and is expressed in the following equation [46]

$$C = (1 \div Y) + (1 \div K_l^2) \tag{6}$$

In the MobileNetV2 architecture, the residual connections are implemented as bottleneck layers, leading to an inverted residual structure. The intermediate expansion layer extracts non-linearity from features by filtering them using lightweight depthwise convolutions. The overall design of MobileNetV2 comprises of 19 residual bottleneck layers after a fully convolution layer with 32 filters at the start [49] The Proposed Model 1 MobileNetV2L2 is built upon the basic block of the MobileNetV2 transfer learning technique. The proposed model's novelty is applying the contrast-limited adaptive Histogram Equalization image enhancement technique (CLAHE) before feeding the dataset to deep learning models. MobileNetV2 is customized by adding 3 dense layers with activation functions such as ReLU and Softmax and freezing all other remaining layers to enhance the model's performance. To further reduce the model's overfitting, the model can perform better on unseen image datasets, dropout of 0.50 and Ridge or L2 Regularization with 0.01 weight is added in the second dense layer.

2) RIDGE OR L2 REGULARIZATION

$L2$ Regularization or Ridge Regularization adds the penality in the loss function. The equation of ridge regularization is given in below equation

$$D = L + \lambda \cdot \Sigma ||w||^2 \tag{7}$$

In above equation D is a cost function, L is a loss function, λ is a penality and w is a slope of the curve. L2 Regularization helps the Deep learning model to prevent overfitting by applying constraints proportional to the sum of the squares of the weights which will help Deep Learning models to learn small weights values and avoid overfitting of the model [58] The regularization function's main purpose is to decrease the overfitting problem in deep learning models. There are two types of Regularization methods Lasso or L1 regularizer and L2 or Ridge Regularizer. Lasso shrinks some less important feature coefficients to zero so some feature is removed whereas Ridge or L2 Regularization does not remove most of the features [58] The confusion matrix of DS1 and DS2 are shown in Figure. 17 and Figure. 18 respectively.

3) PROPOSED MODEL2

Proposed Model2 is shown in Figure. 11. Various Ablation study is done to achieve Proposed Model 2 using customized CNN approach. One Ablation study done here is with change in CNN layers ranging from 3 to 7, shown in table11 and it is observed that customized CNN model with three convolutional layer is performing better. Another Ablation study is performed with various epochs changing the activation function (ReLU and ELU) in second dense layer of customized CNN approach. In normal CNN, there are three convolutional layers, three maxpool layers, and

each convolutional layer uses an activation unit (RELU) with a dropout percentage of 30%. This is named here in this paper as customCNN1. In the modified convolutional layer, three dense layers are employed: the first layer employs Relu as the activation function, while the second layer adds a regularization term in addition to the ELU activation function. The last dense layer employs the softmax function as the activation function and is used for classification and is named as customCNN2. Both customCNN1 and customCNN2 are compared, customCNN2 performed better so base model for proposed model 2 is customCNN2 which is performing better in comparison to other custom CNN models. The novelty of Proposed Model 2 is the introduction of the ELU activation function and the addition of L2 Regularization techniques in customCNN model. Figure. 18 and Figure. 20 shows confusion matrix and training and validation accuracy and loss graph of proposed model2. Table 9 shows performance metrics of customCNN1 model with various epochs change such as 50, 100, 150 and 200 and Table 11 shows performance metrics of customCNN2 model with various epochs change such as 50, 100, 150 and 200 Figure. 12, Figure. 13, Figure. 14 and Figure. 15 shows confusion matrix of customCNN1 model with accuracy 50,100,150,200 respectively. Fig. 21, Figure. 22, Figure. 23 and Figure. 24 shows customCNN1 training accuracy, validation accuracy and training and validation loss for accuracy of 50,100,150,200 respectively. Figure. 12, Figure. 26 and Figure. 27 shows shows confusion matrix of customCNN2 model with accuracy 50, 150 and 200 respectively. Figure. 28, Figure. 29 and Fig. 30 shows training and validation accuracy and loss graph of customCNN2 for epochs 50, 150 and 200 respectively.

4) ELU ACTIVATION FUNCTION

Deep neural networks can learn more quickly and achieve higher classification accuracy because to the "exponential linear unit" (ELU). Like rectified linear units (ReLUs), parametrized ReLUs (PReLUs), leaky ReLUs (LReLUs), and ELUs address the vanishing gradient problem by maintaining the identity for positive values. However, when compared to units with different activation functions, ELUs exhibit better learning properties [60].

IV. RESULTS AND ANALYSIS

The proposed work is providing multi-classification of four most common lung diseases namely Covid19, Tuberculosis, Viral Pneumonia, Bacterial Pneumonia as well as healthy chest X-ray. This work is done for two dataset 5 class and 4 class lung disease classification. This work is done by providing image processing techniques such as image resizing and image augmentation. After image processing, this work is providing comparison among eight existing deep learning techniques. Among these MobileNet is showing better performance in comparison to other employed models.

Various experimentations are performed with major state-of-the-art techniques with and without applying Contrast Limited Adaptive Histogram Equalization techniques (CLAHE) utilizing the DS1 and DS2 dataset mentioned in the dataset section. It is observed from the performance evaluation metrics that MobileNetV2 is performing better in comparison to DenseNet121, InceptionV3, ResNet50, Xception, and InceptionResNetV2. MobileNetV2 deep learning model is utilized in small environments as its operations and memory requirement reduces while accuracy remains the same [49].

TABLE 1. Performance Evaluation of DS1 in terms of accuracy for various deep learning state-of-the-art techniques without applying CLAHE technique.

Architecture	*Accuracy(Training)*	*Accuracy(Validation)*
Shallow CNN	*88.40%*	*82.51%*
VGG-19	*92.10%*	*74.00%*
EfficientNetB0	*85.00%*	*83.51%*
InceptionV3	*90.10%*	*84.20%*
ResNet50	*92.81%*	*81.00%*
DenseNet121	*94.30%*	*83.60%*
Xception	*92.72%*	79.44%
MobileNet	**96.76%**	**86.05%**
InceptionResNetV2	93.90%	*83.10%*
Customdensenet1	97.40%	*86.85%*
Customdensenet2	95.41%	*85.61%*
Customdensenet3	90%	*85.56%*
Custommobilenet1	97.31%	*86.50%*
Custommobilenet2	97.83%	*86.34%*

TABLE 2. Performance Evaluation of DS1 in terms of accuracy for various deep learning state of the art techniques with applying CLAHE technique.

Architecture	*Accuracy(Training)*	*Accuracy(Validation)*
Shallow CNN	*88.42%*	*82.54%*
VGG-19	*92.12%*	*74.80%*
EfficientNetB0	*85.05%*	*83.58%*
InceptionV3	*90.12%*	*84.23%*
ResNet50	*92.88%*	*81.50%*
DenseNet121	*94.31%*	*83.63%*
Xception	*92.73%*	79.46%
MobileNet	**96.76%**	**87.05%**
InceptionResNetV2	91.93%	*84.85%*
Customdensenet1	97.47%	*86.86%*
Customdensenet2	97.47%	*85.86%*
Customdensenet3	90%	*86.56%*
Custommobilenet1	97.32%	*86.52%*
Custommobilenet2	97.84%	*86.36%*

TABLE 3. Performance Evaluation of DS2 in terms of accuracy for various deep learning state of the art techniques.

Architecture	*Accuracy(Training)*	*Accuracy(Validation)*
Shallow CNN	*95.99%*	*93.75%*
VGG-19	*89.76%*	*83.98%*
EfficientNetB0	*44.20%*	*48.12%*
InceptionV3	*92.34%*	*84.47%*
ResNet50	*91.88%*	*82.50%*
DenseNet121	*85.36%*	*82.50%*
Xception	*93.73%*	80.46%
MobileNet	**96.41%**	**96.88%**
InceptionResNetV2	91.93%	*80.85%*
Customdensenet1	97.08%	*90.62%*
Customdensenet2	95.99%	*93.75%*
Customdensenet3	91%	*86.56%*
Custommobilenet1	96.41%	*96.88%*
Custommobilenet2	98.38%	*96.88%*

TABLE 4. Performance Evaluation of MobileNetV2 in terms of accuracy with change in epochs.

Epochs	*Accuracy(Training)*	*Accuracy(Validation)*	*Accuracy(Test)*
50	*96.41%*	*96.88%*	*95.51%*
100	*97.71%*	*96.88%*	*93.29%*
150	*99.53%*	*100.00%*	*95.51%*
200	*98.38%*	*96.88%*	*96.49%*

TABLE 5. Performance Evaluation of customized MobileNetV2 in terms of accuracy with change in number of dense layer without employing Regularizer.

No.of dense layer	*Accuracy(Training)*	*Accuracy(Validation)*
2	*97.32%*	*86.52%*
3	*98.50%*	*91.00%*
4	*92.00%*	*85.51%*
5	*97.84%*	*86.36%*

TABLE 6. Performance Evaluation of customized MobileNetV2 in terms of accuracy with fixed number of dense layer and employing different weights of L2 Regularizer.

L2 Regularizer weight	*Accuracy(Training)*	*Accuracy(Validation)*
.01	*99.53%*	*100%*
.001	*99.27%*	*92.32%*
.0001	*98.02%*	*90.00%*
.00001	*99.26%*	*92.31%*

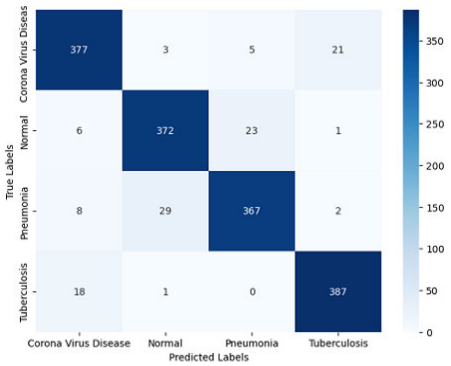

FIGURE 12. Confusion matrix results of customCNN1 model for 50 epochs.

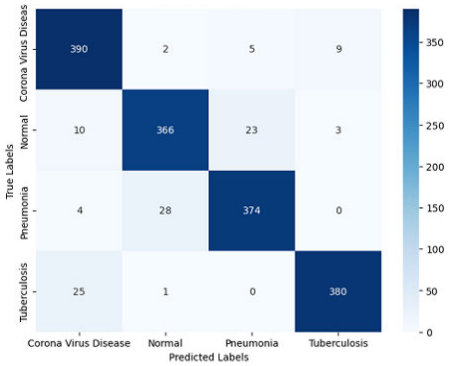

FIGURE 13. Confusion matrix results of customCNN1 model for 100 epochs.

Table 1 and Table 2 utilizes the DS1 dataset to assess performance metrics, including training accuracy and validation accuracy without applying the application of Contrast

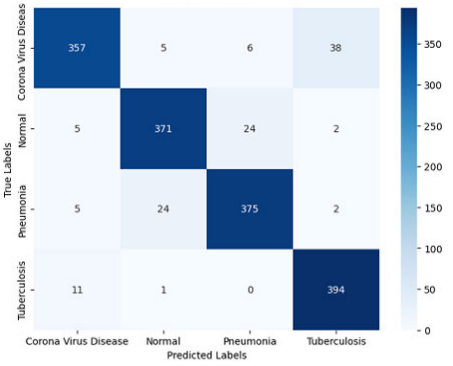

FIGURE 14. Confusion matrix results of customCNN1 model for 150 epochs.

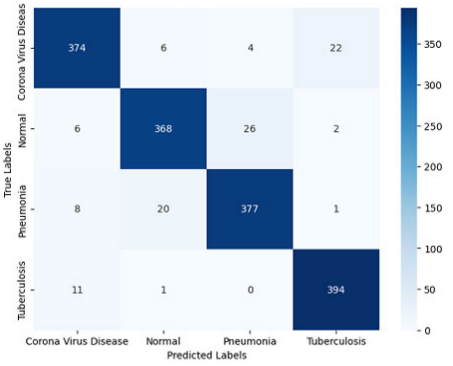

FIGURE 15. Confusion matrix results of customCNN1 model for 200 epochs.

Limited Adaptive Histogram Equalization (CLAHE) techniques and performance metrics of deep learning models after applying the CLAHE techniques to enhance raw X-ray images of lung diseases such as Bacterial Pneumonia, Tuberculosis, Viral Pneumonia, Covid19, and healthy cases. Various deep learning techniques are employed for disease classification, including pre-trained models like DenseNet121, InceptionV3, ResNet50, Xception, MobileNet, and InceptionResNetV2, alongside customized CNN, DenseNet, and MobileNet models aimed at potentially enhancing performance beyond predefined models.

Table 3 is utilizing DS2 to obtain lung diseases classification of Covid19, Pneumonia, Tuberculosis and normal cases. Deep Learning techniques which are applied for classification of lung diseases are pretrained models of DenseNet121, InceptionV3, ResNet50, Xception, MobileNet and InceptionResNetV2 predefined techniques. Customized CNN, Customized dense Net and customized MobileNet techniques are also used aiming for better performance in comparison to predefined models. It is seen from the Table 4 that MobileNetV2 is best performing model for the specified dataset with 150 epochs. Table 7 is showing performance metrics of DS1 for all the utilized deep learning models. Table 8 is showing performance metrics of DS2 for all the utilized deep learning models. Table 9 and Table 11 shows results of customCNN1 and customCNN2 from 50 to 100 epochs respectively.

TABLE 7. Performance metrics for dataset DS1 for all the utilized deep learning models.

Architecture	Accuracy(Training)	Accuracy(Validation)	accuracy(Test)	precision	recall	f1 score
Shallow CNN	88.42%	82.54%	81.48%	83%	83%	83%
VGG19	92.12%	74.80%	73.14%	73%	71%	74%
EfficientNetB0	85.05%	83.58%	82.05%	78%	78.02%	79%
InceptionV3	90.12%	84.23%	82.34%	80%	81%	81%
ResNet50	92.88%	81.50%	80.50%	81%	82%	80%
DenseNet121	93.42%	85.62%	85.62%	84%	81%	83%
Xception	92.73%	79.46%	78.32%	68%	71%	65%
MobileNet	99.10%	87.05%	87.05%	88%	87%	89%
InceptionResNetV2	92.93%	81.85%	81.85%	81%	79%	80%
Customdensenet1	97.47%	86.86%	86.86%	85%	83%	83%
Customdensenet2	93.42%	85.62%	85.62%	84%	82%	83%
Customdensenet3	90%	86.56%	86.81%	85%	83%	84%
Custommobilenet1	97.32%	86.52%	86.52%	86%	84%	85%
Custommobilenet2	97.84%	86.36%	86.36%	84%	83%	84%
Proposed Model1	97.84%	99.61%	96.51%	96%	95%	94%
Proposed Model2	95.84%	94.61%	96.36%	94%	93%	94%

TABLE 8. Performance metrics for dataset DS2 for all the utilized deep learning models.

Architecture	Accuracy(Training)	Accuracy(Validation)	accuracy(Test)	precision	recall	f1 score
Shallow CNN	95.99%	93.75%	92.48%	93%	93%	93%
VGG19	89.76%	83.98%	82.14%	78%	73%	75%
EfficientNetB0	44.20%	48.12%	45.05%	43%	48.02%	42%
InceptionV3	92.34%	84.47%	83.34%	81%	83%	81%
ResNet50	91.88%	82.50%	81.50%	82%	83%	81%
DenseNet121	85.36%	82.50%	86.12%	85%	82%	83%
Xception	93.73%	80.46%	79.32%	69%	72%	70%
MobileNet	96.41%	96.88%	95.51%	93%	92%	90%
InceptionResNetV2	91.93%	80.85%	81.55%	82%	89%	85%
CustomdenseNet1	97.08%	90.62%	93.42%	90%	88%	89%
CustomdenseNet2	95.99%	93.75%	95.57%	91%	90%	91%
CustomdenseNet3	91%	87.56%	87.81%	86%	84%	83%
CustommobileNet1	96.41%	96.88%	95.51%	88%	86%	87%
CustommobileNet2	98.38%	96.88%	96.49%	94%	92%	93%
Proposed Model1	99.53%	100%	95.51%	96%	95%	94%
Proposed Model2	99.53%	96.79%	91.56%	96%	95%	94%

TABLE 9. Performance metrics of customCNN 1 model with Relu+softmax activation function with change in epochs.

Epochs	Training loss	Training Accuracy	Validation loss	Validation Accuracy	Test Loss	Test Accuracy	Precision	Recall	F1-score	ETA
50	0.1613	95.07%	0.2360	92.31%	0.0684	98.09%	93%	93%	93%	148s
100	0.1235	95.45%	0.2857	91.37%	0.1280	96.26%	93%	93%	93%	148s
150	0.2372	94.35%	0.1872	92.06%	0.0296	96.75%	91%	91%	91%	287s
200	0.1372	95.28%	0.2872	90.69%	0.0196	97.04%	93%	93%	93%	228s

TABLE 10. Performance metrics of changing number of dense layer from 3 to 7 with elu+softmax activation function with change in epochs.

No of layers	Training loss	Training Accuracy	Validation loss	Validation Accuracy	Test Loss	Test Accuracy	Precision	Recall	F1-score	ETA
3	0.1231	96.79%	0.3573	91.56%	0.0536	99.26%	92%	92%	92%	144s
4	0.1897	94.60%	0.3367	91.37%	0.0858	98.07%	91%	90%	90%	131s
5	0.2089	93.87%	0.1868	93.81%	0.1120	97.14%	91%	90%	90%	222s
6	0.2515	92.05%	0.2710	91.12%	0.1926	94.57%	92%	92%	92%	203s
7	0.2448	92.57%	0.3175	90.81%	0.1868	94.45%	91%	92%	91%	228s

TABLE 11. Performance metrics of customCNN 2 with elu+softmax activation function with change in epochs.

Epochs	Training loss	Training Accuracy	Validation loss	Validation Accuracy	Test Loss	Test Accuracy	Precision	Recall	F1-score	ETA
50	0.1313	96.38%	0.3502	90.81%	0.0719	98.68%	92%	91%	91%	313s
100	0.1231	96.79%	0.3573	91.56%	0.0536	99.26%	92%	92%	92%	144s
150	0.2553	92.26%	0.3158	90.87%	0.2340	94.41%	91%	91%	91%	137s
200	0.1508	95.34%	0.3640	91.31%	0.1171	97.10%	92%	92%	92%	203s

Figure 16 shows graph representing accuracy of customized DenseNet models namely customdensenet1, customdensenet2 and customdensenet3 deep learning models. Customdensenet1 deep learning model utilizes the

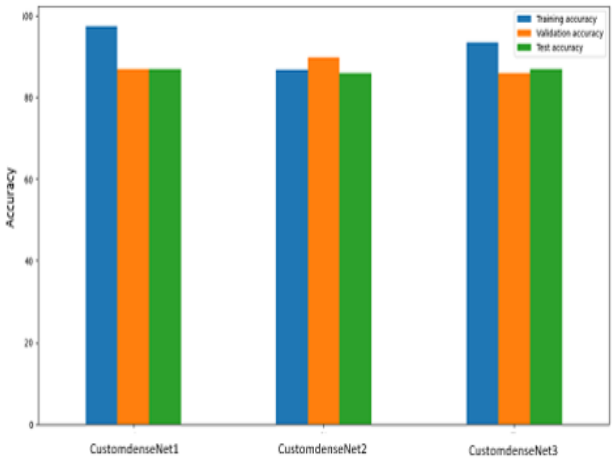

FIGURE 16. Graph of accuracy results for various experimented densenet models.

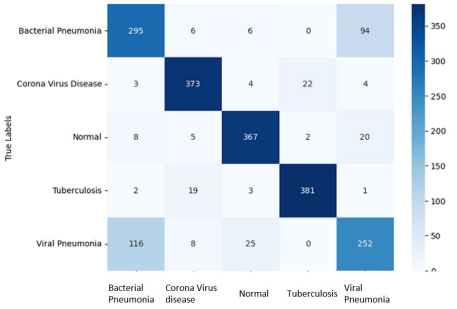

FIGURE 17. Graph of confusion matrix results of proposed model1.

DenseNet transfer learning approach with one extra dropout layer of 0.50 to avoid overfitting. To build a more efficient Deep learning model, two additional dense layers are added, one with 512 neurons and an activation function as ReLU. In contrast, the other Dense layer is used for classification purposes with Softmax as the activation function. Customdensenet2 deep Learning model utilizes the DenseNet transfer learning approach with one extra dropout layer of 0.50 to avoid overfitting. To build a more efficient Deep learning model, three additional dense layers are added, one with 512 neurons and an activation function as ReLU, second dense layer with 128 neuron and ridge regularizer of.01 is added to avoid overfitting. In contrast, the other Dense layer is used for classification purposes with Softmax as the activation function. The state-of-the-art customized DenseNet transfer learning technique is employed by the Customdensenet3 deep learning model. It has one layer with a 0.50 dropout and five additional dense layers for extracting more specific information from the image. The first dense layer uses 512 neurons with Relu acting as the activation function. The second dense layer utilizes 256 neurons with Relu as an activation function, the third dense layer uses 128 neurons with Relu as an activation function, and the fourth dense layer uses 64 neurons with ridge regularizer of.To avoid overfitting, 01 weight is added in this instance.

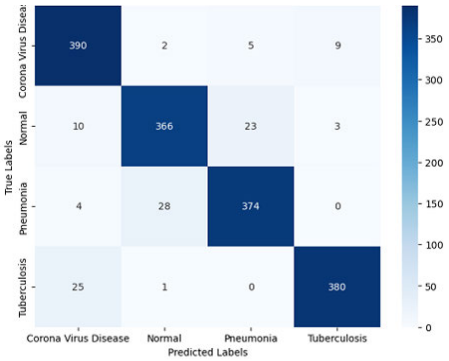

FIGURE 18. Confusion matrix result of Proposed Model2.

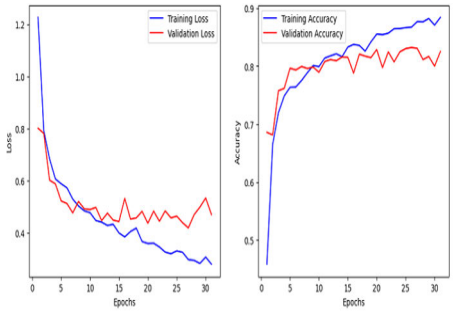

FIGURE 19. Results of the proposed model1 training and validation accuracy and loss graphs.

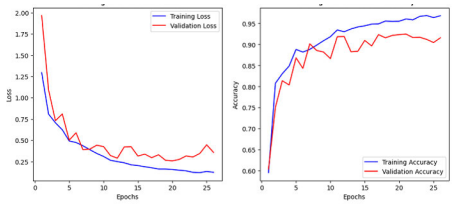

FIGURE 20. Results of the proposed model2 training and validation accuracy and loss graphs.

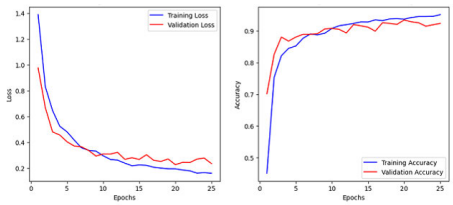

FIGURE 21. Accuracy and loss graph of customCNN1 model for 50 epochs during training and validation.

Fifth and last dense layer is for classification purpose and it is using Softmax as an activation function.

Figure 19 shows graph of training and validation accuracy of proposed model 1. MobileNet model efficiency is enhanced by adding three additional dense layers and freezing all other layers, thereby adapting the MobileNetV2 transfer learning approach. To avoid overfitting, a dropout rate of 50% and Ridge regularization with a coefficient of 0.01 are employed. Additionally, to facilitate multi-classification of specific lung illnesses, a Softmax activation layer is utilized in the last dense layer. This customized

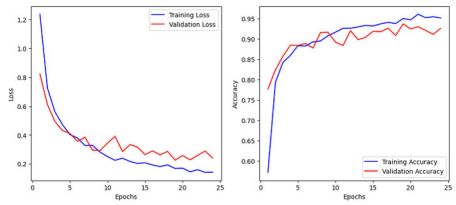

FIGURE 22. Accuracy and loss graph ofustomCNN1 model for 100 epochs during training and validation.

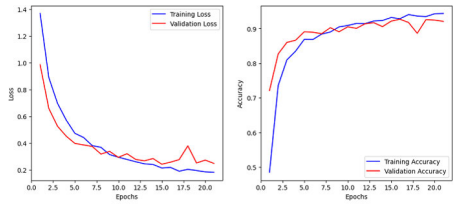

FIGURE 23. Accuracy and loss graph of customCNN1 model for 150 epochs during training and validation.

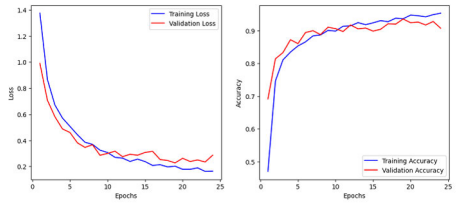

FIGURE 24. Accuracy and loss graph of customCNN1 model for 200 epochs during training and validation.

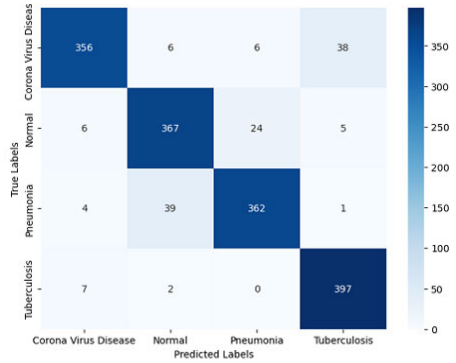

FIGURE 25. Confusion matrix results of customCNN2 model for 50 epochs.

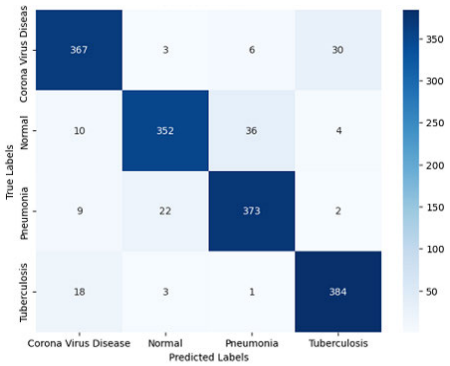

FIGURE 26. Confusion matrix results of customCNN2 model for 150 epochs.

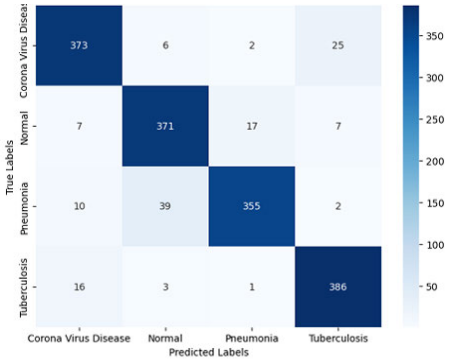

FIGURE 27. Confusion matrix results of customCNN2 model for 200 epochs.

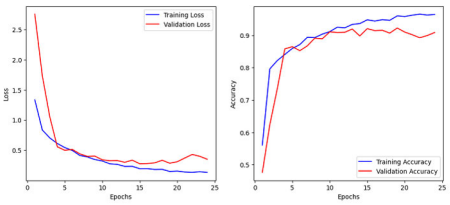

FIGURE 28. Graph of training and validation accuracy and loss results of customCNN2 model for 50 epochs.

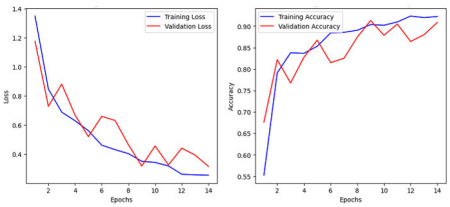

FIGURE 29. Graph of training and validation accuracy and loss results of customCNN2 model for 150 epochs.

model undergoes training for 150 epochs, yielding impressive results indicative of its state-of-the-art performance.

Figure 17, 18, 19, 20 shows training accuracy, validation accuracy, training loss, validation loss and confusion matrix of Proposed Model 1 and Proposed Model 2 respectively.

Figure 21,22,23,24, 12, 13, 14, 15 shows the graph of training accuracy, validation accuracy, traing loss and validation loss and confusion matrix result of custom CNN1 from 50 epochs to 100 epochs respectively.

In Custom CNN 1, there are three convolutional layers, three maxpool layers, and each convolutional layer uses an activation unit (Relu) with a dropout percentage of 30%. The modified convolutional layer uses three dense layers in addition with convolutional layer and maxpool layer. The last dense layer employs the softmax function as the activation function and is used for classification.

From Figures 20, 18, 25, 26, 27, 26, 28, and 29 and 30 shows training and validation accuracy and loss graphical representation and confusion matrix of customCNN2 model results from epoch 50 to 200 respectively. In Custom CNN 2, there are three convolutional layers, three maxpool layers, and each convolutional layer uses an activation unit (Elu) with a dropout percentage of 30%. The modified convolutional

TABLE 12. Comparison of proposed models accuracy with other state-of-the-art approaches.

Paper	Diseases	Architecture	Accuracy
Abobaker Mohammed Qasem Farhan [2]	Bacterial Pneumonia, Viral Pneumonia and normal	HDLA-DNN	98.99%
A. M. Q. Farhan et al. [7]	Normal, Pneumonia, Covid	k-symbol Lerch transcendent functions model + customized CNN	98.60%
Tulin Ozturk et al. [12]	Pneumonia, Covid and normal	DarkCovidNet	87.02%
Xin Zhang et al. [18]	Bacterial Pneumonia, Viral Pneumonia, Covid and normal	CNN+Encoder+Decoder	87.9%
S.-L. Yi et al. [46]	Bacterial Pneumonia, Viral Pneumonia, Tuberculosis, COVID and normal	RedCNN	91.796%
Proposed Model 1 and 2	Bacterial Pneumonia, Viral Pneumonia, Tuberculosis, COVID and normal	MobileNetV2L2, CustomCNN2	95.51% and 99.26%

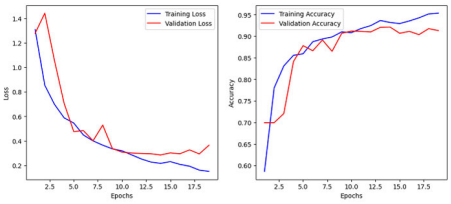

FIGURE 30. Graph of training and validation accuracy and loss results of customCNN2 model for 200 epochs.

layer uses three dense layers in addition with convolutional layer and maxpool layer. The last dense layer employs the softmax function as the activation function and is used for classification. Figure 20 and Figure 18 shows graphical results of proposed Model 2. Proposed Model2 is actually customCNN2 trained for 100 epochs.

Comparison of Proposed models accuracy from other state of the art approaches are as shown in Table 12. The Proposed models showing better accuracy in comparison to state-of-the-art techniques as tabulated in the Table 12.

Based on all observations, it can be concluded that MobileNetV2 achieved better accuracy 0.9676 as training accuracy and 0.8705 as validation accuracy. The proposed model is build on the base of MobileNetV2 by customizing the layers and adding dropout and L2 regularization techniques. The proposed state of the art technique MobileNetV2L2 is showing 99.53% as training accuracy, 99.8% as validation accuracy and 95.51% as test accuracy. Another Proposed Model 2 custom CNN2 is showing 96.79% as training accuracy, 91.56% as validation accuracy and 99.26% as testing accuracy.

V. CONCLUSION

The exploration of lung diseases and their early detection is critical given the potential fatality associated with undetected damage to the lungs. This study proposes two innovative techniques for classifying lung diseases, introducing Proposed Model 1 and Proposed Model 2. Proposed Model 1, featuring a custom mobileNetV2L2, provided training accuracy of 99.53%, validation accuracy of 100%, and test accuracy of 95.51%, demonstrates superior performance compared to other existing techniques. The Proposed Model 2, built on a CNN with unique modifications and exhibits commendable performance across the accuracy metrics. Model 2 provided a training accuracy of 96.79%, validation accuracy of 91.56%, and a testing accuracy of 99.26%. The work carried out with publicly available datasets DS1 and DS2. This research contributes a valuable tool for medical professionals, enabling enhanced diagnosis and serving as a reliable second opinion in the intricate process of identifying and preventing potential lung diseases. In the future, More ablation studies will be done and this work will be extended to adding more lung diseases to the specified datasets to achieve a more efficient deep-learning model that can diagnose lung diseases more precisely and at the earliest. The limitation of this work is that only four Lung diseases (Pneumonia, COVID-19, Lung Cancer, and Tuberculosis) are incorporated in this work. Other lung diseases like Pneumothorax and lung Cancer can be added to the dataset. This work can also be extended with advanced architecture like Vision Transformer.

REFERENCES

[1] F. M. J. M. Shamrat, S. Azam, A. Karim, R. Islam, Z. Tasnim, P. Ghosh, and F. De Boer, "LungNet22: A fine-tuned model for multiclass classification and prediction of lung disease using X-ray images," *J. Pers. Med.*, vol. 12, no. 5, p. 680, Apr. 2022, doi: 10.3390/jpm12050680.

[2] A. M. Q. Farhan and S. Yang, "Automatic lung disease classification from the chest X-ray images using hybrid deep learning algorithm," *Multimedia Tools Appl.*, vol. 82, no. 25, pp. 38561–38587, Mar. 2023, doi: 10.1007/s11042-023-15047-z.

[3] S. Secinaro, D. Calandra, A. Secinaro, V. Muthurangu, and P. Biancone, "The role of artificial intelligence in healthcare: A structured literature review," *BMC Med. Informat. Decis. Making*, vol. 21, no. 1, pp. 1–23, Apr. 2021, doi: 10.1186/s12911-021-01488-9.

[4] D. R. Brenner, J. R. McLaughlin, and R. J. Hung, "Previous lung diseases and lung cancer risk: A systematic review and meta-analysis," *PLoS ONE*, vol. 6, no. 3, Mar. 2011, Art. no. e17479, doi: 10.1371/journal.pone.0017479.

[5] S. P. Power, F. Moloney, M. Twomey, K. James, O. J. O'Connor, and M. M. Maher, "Computed tomography and patient risk: Facts, perceptions and uncertainties," *World J. Radiol.*, vol. 8, no. 12, p. 902, Jan. 2016, doi: 10.4329/wjr.v8.i12.902.

[6] L. Alzubaidi, J. Zhang, A. J. Humaidi, A. Al-Dujaili, Y. Duan, O. Al-Shamma, J. Santamaría, M. A. Fadhel, M. Al-Amidie, and L. Farhan, "Review of deep learning: Concepts, CNN architectures, challenges, applications, future directions," *J. Big Data*, vol. 8, no. 1, pp. 1–74, Mar. 2021, doi: 10.1186/s40537-021-00444-8.

[7] M. H. Al-Sheikh, O. Al Dandan, A. S. Al-Shamayleh, H. A. Jalab, and R. W. Ibrahim, "Multi-class deep learning architecture for classifying lung diseases from chest X-ray and CT images," *Sci. Rep.*, vol. 13, no. 1, Nov. 2023, Art. no. 19373, doi: 10.1038/s41598-023-46147-3.

[8] I. Goodfellow, Y. Bengio, and A. Courville, "Convolutional networks," in *Deep Learning*, vol. 1. Cambridge, MA, USA: MIT Press, 2016, pp. 321–348.

[9] T. Rahman, A. Khandakar, M. A. Kadir, K. R. Islam, K. F. Islam, R. Mazhar, T. Hamid, M. T. Islam, S. Kashem, Z. B. Mahbub, M. A. Ayari, and M. E. H. Chowdhury, "Reliable tuberculosis detection using chest X-ray with deep learning, segmentation and visualization," *IEEE Access*, vol. 8, pp. 191586–191601, 2020, doi: 10.1109/ACCESS.2020.3031384.

[10] C. Shorten and T. M. Khoshgoftaar, "A survey on image data augmentation for deep learning," *J. Big Data*, vol. 6, no. 1, pp. 1–48, Jul. 2019, doi: 10.1186/s40537-019-0197-0.

[11] S. Tammina, "Transfer learning using VGG-16 with deep convolutional neural network for classifying images," *Int. J. Sci. Res. Publications*, vol. 9, no. 10, p. 9420, Oct. 2019, doi: 10.29322/ijsrp.9.10.2019.p9420.

[12] T. Ozturk, M. Talo, E. A. Yildirim, U. B. Baloglu, O. Yildirim, and U. Rajendra Acharya, "Automated detection of COVID-19 cases using deep neural networks with X-ray images," *Comput. Biol. Med.*, vol. 121, Jun. 2020, Art. no. 103792, doi: 10.1016/j.compbiomed.2020.103792.

[13] R. R. Nair and T. Singh, "Multi-sensor, multi-modal medical image fusion for color images: A multi-resolution approach," in *Proc. 10th Int. Conf. Adv. Comput. (ICoAC)*, Chennai, India, Dec. 2018, pp. 249–254, doi: 10.1109/ICoAC44903.2018.8939112.

[14] A. Tripathi, T. Singh, B. Prakash Kn, and K. Rajamani, "Detection of COVID disease using computed tomography images," in *Proc. 14th Int. Conf. Comput. Commun. Netw. Technol. (ICCCNT)*, Delhi, India, Jul. 2023, pp. 1–5, doi: 10.1109/ICCCNT56998.2023.10306637.

[15] A. Krizhevsky, I. Sutskever, and G. E. Hinton, "ImageNet classification with deep convolutional neural networks," *Commun. ACM*, vol. 60, no. 6, pp. 84–90, May 2017, doi: 10.1145/3065386.

[16] A. Halder and B. Datta, "COVID-19 detection from lung CT-scan images using transfer learning approach," *Mach. Learn., Sci. Technol.*, vol. 2, no. 4, Jul. 2021, Art. no. 045013, doi: 10.1088/2632-2153/abf22c.

[17] I. Patel, S. Patel, and A. Patel, "Analysis of various image preprocessing techniques for denoising of flower images," *Int. J. Comput. Sci. Eng.*, vol. 6, no. 5, pp. 1111–1117, May 2018, doi: 10.26438/ijcse/v6i5.11111117.

[18] X. Zhang, L. Han, T. Sobeih, L. Han, N. Dempsey, S. Lechareas, A. Tridente, H. Chen, S. White, and D. Zhang, "CXR-Net: A multitask deep learning network for explainable and accurate diagnosis of COVID-19 pneumonia from chest X-ray images," *IEEE J. Biomed. Health Informat.*, vol. 27, no. 2, pp. 980–991, Feb. 2023, doi: 10.1109/JBHI.2022.3220813.

[19] D. Venugopal, J. Amudha, and C. Jyotsna, "Developing an application using eye tracker," in *Proc. IEEE Int. Conf. Recent Trends Electron., Inf. Commun. Technol. (RTEICT)*, Bengaluru, India, May 2016, pp. 1518–1522, doi: 10.1109/RTEICT.2016.7808086.

[20] C. Szegedy, V. Vanhoucke, S. Ioffe, J. Shlens, and Z. Wojna, "Rethinking the inception architecture for computer vision," in *Proc. IEEE Conf. Comput. Vis. Pattern Recognit. (CVPR)*, Las Vegas, NV, USA, Jun. 2016, pp. 2818–2826, doi: 10.1109/CVPR.2016.308.

[21] M. Tan and Q. Le, "EfficientNet: Rethinking model scaling for convolutional neural networks," in *Proc. Int. Conf. Mach. Learn.*, May 2019, pp. 6105–6114.

[22] M. M. A. Rahhal, Y. Bazi, R. M. Jomaa, M. Zuair, and F. Melgani, "Contrasting EfficientNet, ViT, and gMLP for COVID-19 detection in ultrasound imagery," *J. Personalized Med.*, vol. 12, no. 10, p. 1707, Oct. 2022, doi: 10.3390/jpm12101707.

[23] S. S. Alahmari, B. Altazi, J. Hwang, S. Hawkins, and T. Salem, "A comprehensive review of deep learning-based methods for COVID-19 detection using chest X-ray images," *IEEE Access*, vol. 10, pp. 100763–100785, 2022, doi: 10.1109/ACCESS.2022.3208138.

[24] G. Huang, Z. Liu, L. Van Der Maaten, and K. Q. Weinberger, "Densely connected convolutional networks," in *Proc. IEEE Conf. Comput. Vis. Pattern Recognit. (CVPR)*, Honolulu, HI, USA, Jul. 2017, pp. 2261–2269, doi: 10.1109/CVPR.2017.243.

[25] S. Gite, A. Mishra, and K. Kotecha, "Enhanced lung image segmentation using deep learning," *Neural Comput. Appl.*, vol. 35, no. 31, pp. 22839–22853, Jan. 2022, doi: 10.1007/s00521-021-06719-8.

[26] S. Bharati, P. Podder, and M. R. H. Mondal, "Hybrid deep learning for detecting lung diseases from X-ray images," *Informat. Med. Unlocked*, vol. 20, Jan. 2020, Art. no. 100391, doi: 10.1016/j.imu.2020.100391.

[27] S. Buragadda, K. S. Rani, S. V. Vasantha, and M. K. Chakravarthi, "HCUGAN: Hybrid cyclic UNET GAN for generating augmented synthetic images of chest X-ray images for multi classification of lung diseases," *Int. J. Eng. Trends Technol.*, vol. 70, no. 2, pp. 229–238, Feb. 2022, doi: 10.14445/22315381/ijett-v70i2p227.

[28] A. Das, "Adaptive UNet-based lung segmentation and ensemble learning with CNN-based deep features for automated COVID-19 diagnosis," *Multimedia Tools Appl.*, vol. 81, no. 4, pp. 5407–5441, Dec. 2021, doi: 10.1007/s11042-021-11787-y.

[29] M. Zak and A. Krzyżak, "Classification of lung diseases using deep learning models," in *Proc. Int. Conf. Comput. Sci.* Cham, Switzerland: Springer, Jun. 2020, pp. 621–634.

[30] M. Hong, B. Rim, H. Lee, H. Jang, J. Oh, and S. Choi, "Multi-class classification of lung diseases using CNN models," *Appl. Sci.*, vol. 11, no. 19, p. 9289, Oct. 2021, doi: 10.3390/app11199289.

[31] G. F. C. Campos, S. M. Mastelini, G. J. Aguiar, R. G. Mantovani, L. F. D. Melo, and S. Barbon, "Machine learning hyperparameter selection for contrast limited adaptive histogram equalization," *EURASIP J. Image Video Process.*, vol. 2019, no. 1, pp. 1–18, May 2019, doi: 10.1186/s13640-019-0445-4.

[32] O. Ozdemir, R. L. Russell, and A. A. Berlin, "A 3D probabilistic deep learning system for detection and diagnosis of lung cancer using low-dose CT scans," *IEEE Trans. Med. Imag.*, vol. 39, no. 5, pp. 1419–1429, May 2020, doi: 10.1109/TMI.2019.2947595.

[33] T. A. Khan, A. Fatima, T. Shahzad, Atta-Ur-Rahman, K. Alissa, T. M. Ghazal, M. M. Al-Sakhnini, S. Abbas, M. A. Khan, and A. Ahmed, "Secure IoMT for disease prediction empowered with transfer learning in healthcare 5.0, the concept and case study," *IEEE Access*, vol. 11, pp. 39418–39430, 2023, doi: 10.1109/ACCESS.2023.3266156.

[34] R. C. Gonzalez and R. E. Woods, "Digital image fundamentals," in *Digital Image Processing*, 3rd ed., Chennai, India: Pearson, 2008, pp. 55–65.

[35] R. C. Gonzalez and R. E. Woods, "Digital image fundamentals," in *Intensity Transformations and Spatial Filtering*, 3rd ed. Chennai, India: Pearson, 2008, pp. 120–139.

[36] G. O. Young, "Intensity transformation and spatial filtering," in *Digital Image Processing*, vol. 3, 3rd ed., J. Peters, Ed., New York, NY, USA: McGraw-Hill, 2008, pp. 107–139.

[37] A. Tripathi, T. Singh, and R. R. Nair, "Optimal pneumonia detection using convolutional neural networks from X-ray images," in *Proc. 12th Int. Conf. Comput. Commun. Netw. Technol. (ICCCNT)*, Kharagpur, India, Jul. 2021, pp. 1–6, doi: 10.1109/ICCCNT51525.2021.9580140.

[38] H. Mukherjee, S. Ghosh, A. Dhar, S. M. Obaidullah, K. C. Santosh, and K. Roy, "Shallow convolutional neural network for COVID-19 outbreak screening using chest X-rays," *Cognit. Comput.*, vol. 16, no. 4, pp. 1695–1708, Feb. 2021, doi: 10.1007/s12559-020-09775-9.

[39] M. Bansal, M. Kumar, M. Sachdeva, and A. Mittal, "Transfer learning for image classification using VGG19: Caltech-101 image data set," *J. Ambient Intell. Humanized Comput.*, vol. 14, no. 4, pp. 3609–3620, Sep. 2021, doi: 10.1007/s12652-021-03488-z.

[40] F. Chollet, "Xception: Deep learning with depthwise separable convolutions," in *Proc. IEEE Conf. Comput. Vis. Pattern Recognit. (CVPR)*, Honolulu, HI, USA, Jul. 2017, pp. 1800–1807, doi: 10.1109/CVPR.2017.195.

[41] J. Ryu, "A visual saliency-based neural network architecture for no-reference image quality assessment," *Appl. Sci.*, vol. 12, no. 19, p. 9567, Sep. 2022, doi: 10.3390/app12199567.

[42] A. Shazia, T. Z. Xuan, J. H. Chuah, J. Usman, P. Qian, and K. W. Lai, "A comparative study of multiple neural network for detection of COVID-19 on chest X-ray," *EURASIP J. Adv. Signal Process.*, vol. 2021, no. 1, pp. 1–16, Jul. 2021, doi: 10.1186/s13634-021-00755-1.

[43] A. Tripathi, A. Basavapattana, R. R. Nair, and T. Singh, "Visualization of COVID bimodal scan using DNN," in *Proc. 12th Int. Conf. Comput. Commun. Netw. Technol. (ICCCNT)*, Kharagpur, India, Jul. 2021, pp. 1–7, doi: 10.1109/ICCCNT51525.2021.9579878.

[44] H. Wang, H. Jia, L. Lu, and Y. Xia, "Thorax-net: An attention regularized deep neural network for classification of thoracic diseases on chest radiography," *IEEE J. Biomed. Health Informat.*, vol. 24, no. 2, pp. 475–485, Feb. 2020, doi: 10.1109/JBHI.2019.2928369.

[45] S.-L. Yi, S.-L. Qin, F.-R. She, and T.-W. Wang, "RED-CNN: The multi-classification network for pulmonary diseases," *Electronics*, vol. 11, no. 18, p. 2896, Sep. 2022, doi: 10.3390/electronics11182896.

[46] A. G. Howard, M. Zhu, B. Chen, D. Kalenichenko, W. Wang, T. Weyand, M. Andreetto, and H. Adam, "MobileNets: Efficient convolutional neural networks for mobile vision applications," 2017, *arXiv:1704.04861*.

[47] R. Gayathri, P. B. Pati, T. Singh, and R. R. Nair, "A framework for the prediction of diabtetes mellitus using hyper-parameter tuned XGBoost classifier," in *Proc. 13th Int. Conf. Comput. Commun. Netw. Technol. (ICCCNT)*, Kharagpur, India, Oct. 2022, pp. 1–5, doi: 10.1109/ICCCNT54827.2022.9984315.

[48] N. Srivastava, G. Hinton, A. Krizhevsky, I. Sutskever, and R. Salakhutdinov, "Dropout: A simple way to prevent neural networks from overfitting," *J. Mach. Learn. Res.*, vol. 15, no. 1, pp. 1929–1958, 2021.

[49] M. Sandler, A. Howard, M. Zhu, A. Zhmoginov, and L.-C. Chen, "MobileNetV2: Inverted residuals and linear bottlenecks," in *Proc. IEEE/CVF Conf. Comput. Vis. Pattern Recognit.*, Salt Lake City, UT, USA, Jun. 2018, pp. 4510–4520, doi: 10.1109/CVPR.2018.00474.

[50] L. Venkataramana, D. V. V. Prasad, S. Saraswathi, C. M. Mithumary, R. Karthikeyan, and N. Monika, "Classification of COVID-19 from tuberculosis and pneumonia using deep learning techniques," *Med. Biol. Eng. Comput.*, vol. 60, no. 9, pp. 2681–2691, Jul. 2022, doi: 10.1007/s11517-022-02632-x.

[51] S. Goyal and R. Singh, "Detection and classification of lung diseases for pneumonia and COVID-19 using machine and deep learning techniques," *J. Ambient Intell. Humanized Comput.*, vol. 14, no. 4, pp. 3239–3259, Sep. 2021, doi: 10.1007/s12652-021-03464-7.

[52] F. J. M. Shamrat, S. Azam, A. Karim, K. Ahmed, F. M. Bui, and F. De Boer, "High-precision multiclass classification of lung disease through customized MobileNetV2 from chest X-ray images," *Comput. Biol. Med.*, vol. 155, Mar. 2023, Art. no. 106646, doi: 10.1016/j.compbiomed.2023.106646.

[53] B. Saju, N. Tressa, R. K. Dhanaraj, S. Tharewal, J. C. Mathew, and D. Pelusi, "Effective multi-class lung disease classification using the hybrid feature engineering mechanism," *Math. Biosci. Eng.*, vol. 20, no. 11, pp. 20245–20273, 2023.

[54] M. Shimja and K. Kartheeban, "Empowering diagnosis: An astonishing deep transfer learning approach with fine tuning for precise lung disease classification from CXR images," *Automatika*, vol. 65, no. 1, pp. 192–205, Jan. 2024.

[55] A. M. Shaker and S. Xiong, "Lung image classification based on long-short term memory recurrent neural network," *J. Phys., Conf. Ser.*, vol. 2467, no. 1, May 2023, Art. no. 012007.

[56] D.-A. Clevert, T. Unterthiner, and S. Hochreiter, "Fast and accurate deep network learning by exponential linear units (ELUs)," 2015, *arXiv:1511.07289*.

[57] I. Salehin and D.-K. Kang, "A review on dropout regularization approaches for deep neural networks within the scholarly domain," *Electronics*, vol. 12, no. 14, p. 3106, Jul. 2023.

[58] J. Kolluri, V. K. Kotte, M. S. B. Phridviraj, and S. Razia, "Reducing overfitting problem in machine learning using novel L1/4 regularization method," in *Proc. 4th Int. Conf. Trends Electron. Informat. (ICOEI)*, Tirunelveli, India, Jun. 2020, pp. 934–938, doi: 10.1109/ICOEI48184.2020.9142992.

[59] O. M. Dalvi. (2018). *Lung Disease Dataset (4 Types)*. [Online]. Available: https://www.kaggle.com/datasets/omkarmanohardalvi/lungs-disease-dataset-4-types

[60] (2018). *Dataset 2: Samuel, Lung Diseases X-Rays (Grayscale)*. [Online]. Available: https://www.kaggle.com/datasets/samuel156/lungxrays-grayscale

AMRITA TRIPATHI received the Bachelor of Engineering (B.Tech.) degree from the Institute of Technology and Management (ITM), Gorakhpur, in 2006, and the M.Tech. degree from the Madan Mohan Malaviya Engineering College, Gorakhpur, in 2010. She is currently pursuing the Ph.D. degree with the Department of Computer Science and Engineering, Amrita Vishwa Vidyapeetham, Bengaluru. Before the Ph.D. degree, she was an Assistant Professor with the D. J. Sanghvi College of Engineering, Mumbai. Her research interests include digital image processing (disease classification), artificial intelligence, and data science. She published three conference papers in the area of lung disease classification.

TRIPTY SINGH (Senior Member, IEEE) received the B.Tech. degree from DAVV, Indore, in 2000, the M.Tech degree from IIITM Gwalior, in 2004, and the Doctor of Philosophy degree from RGTU, Bhopal, in 2013. She was a Lecturer with ITM Gwalior, MITS, MVJCE, and EPCEW Bengaluru, from 2000 to 2007, from 2008 to 2010, from 2010 to 2011, and from 2011 to 2012, respectively. She was a Guest Faculty Member with the University at Buffalo, Buffalo, NY, USA. She has been a Professor with the Amrita School of Engineering, Bengaluru, since 2012. She is currently an Associate Professor with the Department of Computer Science and Engineering, Amrita School of Computing, Bengaluru, Amrita Vishwa Vidyapeetham, India. She is specifically working on oncology quantification, DCE-MRI, medical image registration, and medical image fusion. Her research interests include digital image processing (medical), artificial intelligence, machine learning, computer vision, soft computing, parallel and distributed systems, ad-hoc networks, network security, and digital systems. She has to her credit more than 60 publications, conducted eight workshops, and was program chairs for seven international conferences in London and India. She was awarded the Best Idea Award in the Best Brain in Bengaluru (3Bs) Contest, the Young International Investigator Award, in 2013 organized by IRNET India and Springer, ISBN No: 978-93-82208-71-6, and the Best Paper Presentation and Best Contains in the Track, in 2013 organized by IRNET India and Springer, ISBN No: 978-93-82208-71-6. She has given invited guest lectures as part of international conferences in machine learning, medical image analysis, medical image registration, pattern classification, both in India and Abroad. She is also a reviewer of many reputed journals. She has also given pre-conference tutorial talks at IEEE and Springer international conferences.

REKHA R. NAIR (Member, IEEE) received the B.C.A. and M.C.A. degrees from Indira Gandhi National Open University, Delhi, in 2011 and 2013, respectively, and the Doctor of Philosophy degree from Amrita School of Engineering, Bengaluru, in 2021. She is currently an Assistant Professor with the Department of Computer Science and Engineering, Alliance University, Bengaluru. She is specifically working on medical image registration, medical image fusion, prediction, and forecasting. She has to her credit more than 50 publications and five patents. Her research interests include digital image processing (medical), artificial intelligence, data science, machine learning, blockchain, the IoT, computer vision, soft computing, and data structure. She was awarded the Best Paper Award in IEEE and Springer conferences.

PRAKASH DURAISAMY (Senior Member, IEEE) received the B.E. degree in electronics and communication engineering from Bharathiar University, in 2002, the M.S.E.E. degree in electrical engineering from the University of South Alabama, USA, in 2008, and the Doctor of Philosophy (Ph.D.) degree in computer science and engineering from the University of North Texas, in 2012. He was a Visiting Scientist with Massachusetts Institute of Technology (MIT). He is an Assistant Professor with the Computer Science Department, University of Wisconsin-Green Bay. His research interests include computer vision, computer graphics, LiDAR, robotics, and biomedical. He is an Early Career Professional Member of IEEE and SPIE. He was involved in organizing various IEEE conferences in India. He serves as the Conference Co-Chair for the 4th ICCCNT Conference in India, Since July 2013, which is technically sponsored by the IEEE Computer Society.